

Original article

Effect of TiO_2 – SiO_2 hybrid nanofluids on enhanced oil recovery process under different wettability conditions

Afshin Goharzadeh¹*, Yap Yit Fatt¹, Jitendra S. Sangwai²

¹Mechanical Engineering Department, Khalifa University of Science and Technology, Abu Dhabi 127788, United Arab Emirates

²Department of Chemical Engineering, Indian Institute of Technology Madras, Chennai 600036, India

Keywords:

Enhanced oil recovery
hybrid nanofluids
wettability
micro-porous media
contact angle

Cited as:

Goharzadeh, A., Fatt, Y. Y., Sangwai, J. S. Effect of TiO_2 – SiO_2 hybrid nanofluids on enhanced oil recovery process under different wettability conditions. *Capillarity*, 2023, 8(1): 1-10. <https://doi.org/10.46690/capi.2023.07.01>

Abstract:

The effect of TiO_2 – SiO_2 hybrid nanofluid on the enhanced oil recovery process is experimentally investigated. The flooding efficiency is measured for a flooding process in an initially oil-filled transparent micro-porous medium. Measurements were performed for two different surface wettability conditions, namely water-wet and neutral-wet. The average nanoparticle size, viscosity, surface tension, and contact angle of TiO_2 – SiO_2 hybrid nanofluid are reported. The flooding efficiency of the hybrid nanofluid is compared with that of SiO_2 nanofluid and TiO_2 nanofluid. The experimental results reveal that for neutral-wet surface condition, SiO_2 nanofluid achieves the best recovery, whereas for water-wet surface condition, TiO_2 – SiO_2 hybrid nanofluid produces the best flooding efficiency. Obtained results showed that TiO_2 nanofluid is unstable, with larger aggregated particles settling under gravity, and therefore not suitable for the flooding process by itself. The efficiency of hybrid nanofluid flooding depends significantly on fluid stability, wettability of the porous wall, surface tension, and contact angle of the three phases (crude oil, nanofluid solution, and solid surface). The TiO_2 – SiO_2 hybrid nanofluid reduces surface tension while increasing contact angle and solution stability.

1. Introduction

Energy demand is rising as the global economy expands at an exponential rate. Therefore, it is essential to create new technologies in order to maintain a consistent supply of oil. Nanotechnology has the potential to revolutionize enhanced oil recovery (EOR) process by modifying the oil reservoir's characteristics (Negin et al., 2016; Alwated and El-Amin, 2021; Sircar et al., 2022). Nanoparticles with a size of 1–100 nm have a high surface-to-volume ratio, a high chemical reactivity, and are able to travel through tiny pores (Li et al., 2018; Cheraghian et al., 2020). Nanofluid flooding is a low-cost chemical flooding technique, which alters the properties of the flooding fluid through the addition of low-volume concentration nanoparticles (Alomair et al., 2014; Salem Ragab and Hannora, 2015). Recent studies found that the addition of nanoparticles in the flooding fluid can alter the wettability

of the reservoir (Li et al., 2017; Yuan et al., 2021), reduce pore blockage by preventing asphaltene deposition (Sun et al., 2017), change the disjoining pressure (McElfresh et al., 2012; Moghadasi et al., 2019), decrease interfacial tension (Liu et al., 2017), and enhance the rheology of the flooding fluid (Chaturvedi et al., 2021).

When two or more types of nanoparticles are homogenized in a liquid, the resulting fluid mixture, known as hybrid nanofluid, can have properties very different from those of the original base fluid. By varying the types and amounts of nanoparticles added to the original base fluid, a hybrid nanofluid can be developed for various engineering applications.

The positive effect of hybrid nanofluids in the engineering process was initially demonstrated through studies of heat transfer enhancement (Suresh et al., 2011; Mukherjee et al.,

2022). Previous studies show that hybrid nanofluids have higher stability compared to nanofluids with only one type of nanoparticles. Suresh et al. (2011) measured the thermal conductivity of Al_2O_3 -Cu hybrid nanofluid and observed a maximum enhancement of 12.11% for a volume concentration of 2%. Yarmand et al. (2016) investigated the thermal conductivity of graphene nanoplatelet/platinum hybrid nanofluid and measured a 17% enhancement of the thermal conductivity compared to the original base fluid. Minea (2017) numerically studied the thermal conductivity of hybrid nanofluids with different combinations of Al_2O_3 , SiO_2 , and TiO_2 nanoparticles. His numerical prediction shows an overall increase in thermal conductivity for all hybrid nanofluids with a maximum enhancement of 12% compared to the base fluid. Bahrami et al. (2016) studied the rheological behavior of hybrid nanofluids with iron and copper nanoparticles. They observed that the viscosity of the solution depends on its nanoparticle concentration, exhibiting Newtonian behavior for a low concentration (less than 0.1%) and non-Newtonian behavior for a high concentration (more than 0.25%). Madhesh et al. (2014) studied the convective heat transfer and rheological characteristics of Cu- TiO_2 hybrid nanofluids. Their experimental results revealed that the convective heat transfer coefficient, Nusselt number, and overall heat transfer coefficient were increased by 52%, 49%, and 68%, respectively, for 1.0% volume nanoparticle concentration. Sivasankaran and Bhuvaneshwari (2022) studied the thermal performance index of the heat exchangers filled with hybrid nanofluid and porous media. They used TiO_2 - Al_2O_3 hybrid fluid and concluded that the hybrid nanofluid improved the heat transfer coefficient relative to nanofluid by 4%-6% and increased the pressure loss relative to nanofluid by 9%-11%. Mukherjee et al. (2022) experimentally studied the thermo-fluidic performance of SiO_2 -ZnO hybrid nanofluid on the enhancement of heat transport in a tube. They observed that the hybrid nanofluid increases the convective heat transfer coefficient by a maximum of 29% compared to pure water. To improve oil recovery, Kashefi et al. (2023) investigated the effect of graphene oxide-silica (GO- SiO_2) hybrid nanofluid on the wettability of sandstone oil reservoirs. They noticed that the contact angle increased from 23 degrees (on an untreated surface) to 161 degrees at a nanoparticle concentration of 0.015 wt%. They concluded that GO- SiO_2 hybrid nanofluid has the potential to be used as an affordable, adaptable, and eco-friendly natural flooding fluid for the EOR process.

Among different types of nanoparticles, nanofluids with SiO_2 or TiO_2 nanoparticles have demonstrated tremendous potential in heat transfer, enhanced oil recovery, and well-drilling processes. However, to the authors' knowledge, only a few studies on the use of SiO_2 - TiO_2 hybrid nanofluids in EOR are reported (Kazemzadeh et al., 2018; Ali et al., 2021). Ali et al. (2021) developed a new engineered water-based hybrid nanofluid with TiO_2 - SiO_2 -polyacrylamide nanocomposites for EOR applications. They observed that when the hybrid nanofluid is added to smart water, the resulting mixture has a 65% reduction in interfacial tension, a 32% change in wettability, and more importantly, a 10.5% increase in oil recovery. Kazemzadeh et al. (2018) investigated the use

of flooding fluid containing TiO_2 - SiO_2 nanocomposites in EOR processes at different pressures. They concluded that at the intermediate pressure (1,500 bar), wettability alteration due to the presence of TiO_2 - SiO_2 nanocomposites is the dominant mechanism in achieving an improved recovery of approximately 72%.

Meanwhile, several researchers have made efforts to measure the thermal properties of SiO_2 - TiO_2 hybrid nanofluids (Hamid et al., 2018; Azmi et al., 2021). Azmi et al. (2021) studied the thermal performance of TiO_2 - SiO_2 nanofluids in a tube with wire coil inserts. They concluded that heat transfer was improved by up to 211.75%. Zainon and Azmi (2021) investigated the thermal properties of water-bioglycol- TiO_2 - SiO_2 hybrid nanofluids. They observed that the thermal conductivity of the hybrid nanofluid was increased by 12.52% compared to the original water-bioglycol mixture. Nabil et al. (2017) used a water-ethylene glycol- TiO_2 - SiO_2 hybrid nanofluid with a water to ethylene glycol volume ratio of 60:40. They observed that the thermal conductivity of water-ethylene glycol- TiO_2 - SiO_2 nanofluid was 22.8% higher than the based water-ethylene glycol fluid for a 3.0% volume concentration and a temperature of 80 °C. Also, they concluded that the viscosity was affected by nanoparticle concentration and temperature. Hamid et al. (2018) concluded that the thermal conductivity of TiO_2 - SiO_2 hybrid nanofluid is up to 16% higher than the base fluid. The thermal properties of TiO_2 - SiO_2 hybrid nanofluids are well reported in the literature. However, experimental results on the physical properties of TiO_2 - SiO_2 hybrid nanofluid essential in EOR are not available from previous studies.

In previous work, Goharzadeh and Fatt (2022) characterized the properties of SiO_2 nanofluid and quantified its flooding efficiency in an initially oil-filled micro-porous medium of two different surface wettability conditions, i.e., water-wet and neutral-wet. It was found that the best oil recovery process occurred when the SiO_2 nanofluid flooding was used in a neutral-wet surface condition. The present study extends Goharzadeh and Fatt (2022) investigation into TiO_2 - SiO_2 hybrid nanofluid flooding. This work provides two sets of experimental data: (1) measurements of viscosity, density, surface tension, contact angle, and particle size of TiO_2 - SiO_2 hybrid nanofluids; (2) the effect of the mentioned hybrid nanofluid on flooding, subjected to different experimental conditions, such as liquid flowrates and wettability of porous matrix. The obtained measurements complete previous studies by providing essential physical properties of TiO_2 - SiO_2 hybrid nanofluid and the optimum condition in which the hybrid nanofluid is the most suitable working fluid to improve the EOR process. In this paper, the experimental setup, oil properties, and nanofluid preparation are presented in Section 2. The experimental results of this study are presented in Section 3, which contains measurements of the average particle size, viscosity, surface tension, and stability contact angle of nanofluids. Furthermore, the effect of hybrid nanofluids on the flooding process inside the microporous media is presented. Finally, discussions on the role of hybrid nanofluid's physical parameters on flooding efficiency are presented in Section 4.

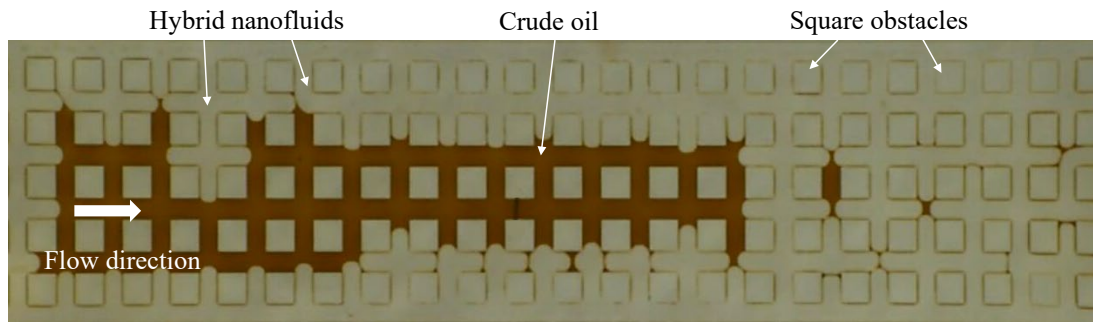


Fig. 1. Image of a microchannel with crude oil residual during hybrid nanofluid flooding.

Table 1. Properties of micromodel used in the experiment.

Parameter	Micromodel
Length (μm)	7,050
Width (μm)	1,500
Depth (μm)	35
Pore volume (μL)	0.26
Permeability (μm^2)	75.49
Porosity (%)	70

Table 2. Crude oil properties.

Properties	Values
API gravity ($^{\circ}\text{API}$)	36.5
Density at 20 $^{\circ}\text{C}$ (g/cc)	0.8406
Kinematic viscosity (cSt)	6.521
Saturates (wt%)	49.9
Aromatics (wt%)	14.2
Resins (wt%)	5.6
Asphaltene (wt%)	0.40

2. Experimental methods

2.1 Experimental setup

The experimental setup, the flow visualization system, and the properties of the crude oil used in this study have been described in our previous study (Goharzadeh and Fatt, 2022). The experimental setup consists of a transparent microchannel with arrays of square obstacles sized $165 \times 165 \mu\text{m}^2$, a syringe pump (Cole-Parmer), a collection tank, and a microscope for flow visualization. The syringe pump is used to inject crude oil or $\text{TiO}_2\text{-SiO}_2$ hybrid nanofluid into the microchannel. The flowrate of the syringe pump ranges from 0.0004 $\mu\text{L/h}$ to 106.6 mL/h. For water flooding, which is compared with nanofluid flooding, the averaged velocity of the water-crude oil front (before the breakthrough) is approximately 0.02 mm/s, corresponding, to a capillary number (Ca) of 4.3×10^{-7} . After centrifuging, crude oil was injected into the micromodel from the inlet tube using the syringe pump. Once the micromodel is filled with crude oil, $\text{TiO}_2\text{-SiO}_2$ hybrid nanofluid is injected at a flowrate of 0.01 mL/h until a breakthrough occurs. In order to further study the flooding process after breakthrough, the flowrate of $\text{TiO}_2\text{-SiO}_2$ hybrid nanofluid is increased by 0.01 mL/h every 6 min until 0.1 mL/h (Fig. 1). During injection processes, oil saturation was monitored by taking high-resolution images. A new microchannel is used in every experiment run and disposed after the experiment. The dimensions of the microchannel are reported in Table 1.

2.2 Properties of the crude oil

In order to prevent the asphaltene and impurities in the crude oil from blocking the micromodel, a centrifuge (SCT-

SPIN-3 Scientific Chemical Technologies, LLC) was used to remove those particles before the flooding experiment. Crude oil was centrifuged at a speed of 5,000 rpm for 20 minutes, and the top layer was used for the flooding experiment. Physico-chemical properties of the crude oil are described in detail in Zhuang's study (Zhuang et al., 2016, 2018), and for convenience, key properties of crude oil are reported in Table 2.

2.3 Nanofluid preparation

There are currently two main techniques to prepare a nanofluid solution: the one-step technique and the two-step technique. The preparation and dispersion of nanoparticles are done simultaneously in a one-step technique. The agglomeration of the particles can be reduced using this method. However, it is expensive and unable to produce nanofluids on a large scale. The most popular technique for preparing nanofluids on a large scale is the two-step technique. In this process, dry nanoparticles were initially mixed with water. A magnetic stirrer and sonicator will then be used to disperse the power into the solution. This approach is cost-effective and has already seen widespread use in the industrial sector (Zhuang et al., 2018).

In this experiment, a stirrer (Stuart SB162) was used to stir nanoparticles in liquid for 20 minutes at a speed of 1,000 rpm. In order to further disperse the nanoparticles in the liquid, a sonicator is used to process the mixture. The samples were placed in a beaker and treated by sonication for 40 minutes at 80% amplitude. The concentration and density of working fluids are reported in Table 3.

Table 3. Working fluids used at room temperature (22 °C).

Material	Concentration	Density (g/cm ³)
DI-Water	0	0.9978
Brine (NaCl)	3 wt%	1.0184
SiO ₂ + brine	0.05 wt% + 3 wt%	1.0198
TiO ₂ + brine	0.05 wt% + 3 wt%	1.0201
TiO ₂ + SiO ₂ + brine	0.05 wt% + 0.05 wt% + 3 wt%	1.0206

Table 4. Size of nanoparticles.

Nanofluid	Average size in liquid solution (nm)	Original size in powder (nm)
SiO ₂	187	12
TiO ₂	1,131	20-40
TiO ₂ -SiO ₂ hybrid	917.8	-

Table 5. The viscosity of flooding fluid (23.5 °C).

Fluid	Dynamic viscosity (mPa·s)
DI-water	0.93
NaCl solution	0.96
SiO ₂ + brine	1.03
TiO ₂ + brine	0.98
TiO ₂ -SiO ₂ + brine	1.01

3. Experimental results

3.1 Particle size of hybrid nanofluid

The average particle size in SiO₂ nanofluid, TiO₂ nanofluid, and TiO₂-SiO₂ hybrid nanofluid is measured using Zetasizer Nano ZS. The average particle sizes of these three nanofluids are presented in Table 4. It can be observed that TiO₂ and SiO₂ nanofluids have, respectively, the largest and smallest particle sizes. The particle size of the TiO₂-SiO₂ hybrid nanofluid is 4.9 times larger than that of the SiO₂ nanofluid particle size but is 1.2 times smaller than that of the TiO₂ nanofluid.

3.2 Viscosity of flooding fluids

A sinusoidal oscillatory viscometer, SV-10, was used to measure the dynamic viscosity of flooding fluids. The viscosity is determined by measuring the driving current of a constant vibration with a fixed frequency and amplitude. The proportional relationship between the driving current and the viscosity can be used to calculate the viscosity. The viscometer dynamically measures the liquid viscosity from 0.3-10,000 cP. During the measurement, the liquid temperature remains con-

Table 6. Surface tension for working fluids.

Working fluid	Surface tension (mN/m)
DI water	71.28
(NaCl) solution	74.06
SiO ₂ + brine	76.76
TiO ₂ + brine	72.67
TiO ₂ -SiO ₂ + brine (power mixing)	72.35
TiO ₂ -SiO ₂ + brine (liquid mixing)	72.69

stant. The size of the viscosity sensor plate is 4 mm and does not cause deformation of the sample. Therefore, non-Newtonian liquids can be measured in a stable manner. Temperature sensors are installed between two viscosity sensor plates, allowing the instrument to correctly reflect the relationships between the measured liquid viscosity and temperature. The dynamic viscosity of flooding fluids is reported in Table 5. It can be noticed that the addition of nanoparticles to the brine solution increases the viscosity. The viscosity of hybrid nanofluid is similar to that of single nanofluids, containing only one type of nanoparticle.

3.3 Surface tension of flooding fluids

The surface tension of nanofluid is measured using the drop volume method (Wilkinson and Kidwell, 1971; Miller and Fainerman, 1998). A high-speed camera is placed in front of the needle to capture the falling droplets. When droplets below the needle become uniform and stable, the recording process starts (Fig. 2). The last recorded image before the detachment of liquid droplet from the needle was selected for analysis (Fig. 2(b)). Using image processing, the volume of the droplet is measured, and the corresponding surface tension is calculated.

Table 6 shows the value of surface tension of different nanofluids compared with that of DI-water and brine solution. When SiO₂ nanoparticles were added to the brine solution, the surface tension increased from 74.06-76.76 mN/m. This addition of nanoparticles alters the surface energy at the liquid-gas interface, which leads to a change in surface tension (Yu and Xie, 2012). When nanoparticles are added to the liquid, they tend to accumulate at the gas-liquid interface, i.e., the concentration near the interface is much higher than that inside the liquid. The Van der Waals force between particles

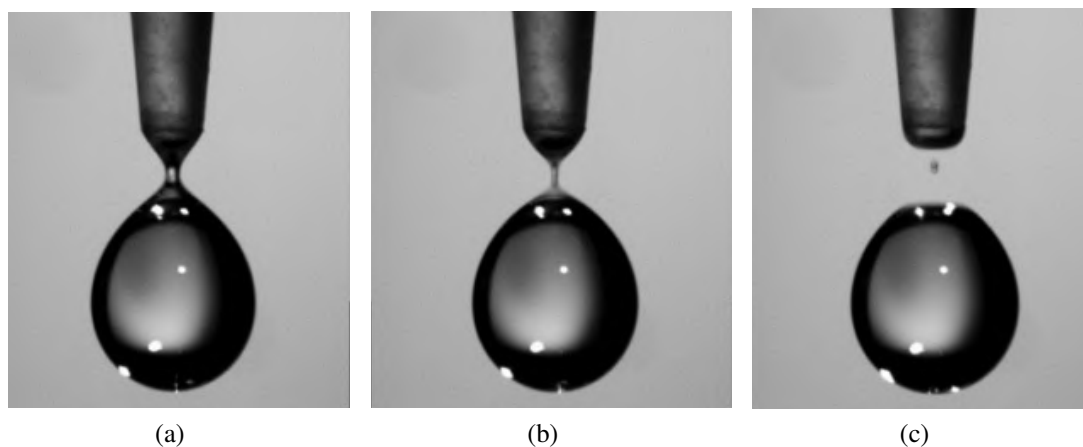


Fig. 2. Falling of a droplet: (a) $t = 0$ ms, (b) $t = 0.5$ ms and (c) $t = 1$ ms.

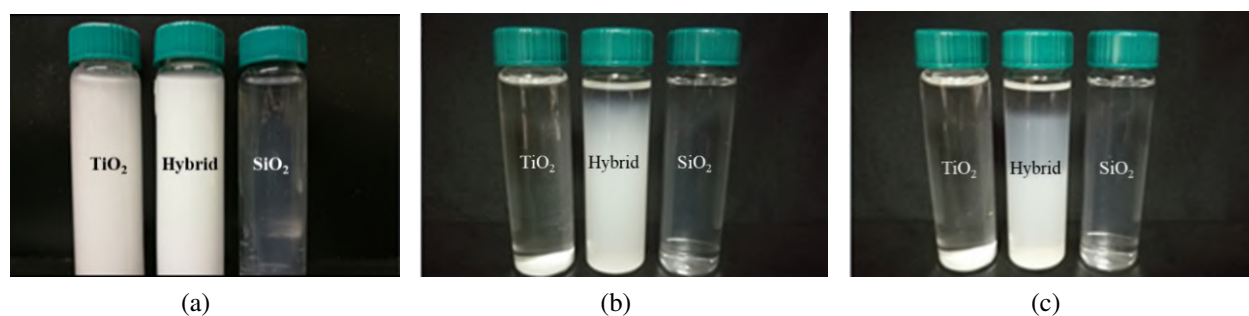


Fig. 3. Stability of nanofluids with time: (a) $t = 0$ h, (b) $t = 96$ h and (c) $t = 192$ h.

at the liquid-gas interface increases the interfacial energy and thus increases surface tension (Radiom et al., 2009; Vafaei et al., 2009). However, compared with SiO_2 nanoparticles, the surface tension of the brine decreased from 74.06-72.67 mN/m after the addition of TiO_2 nanoparticles. Both Murshed et al. (2008) and Radiom et al. (2009) quantified similar trends using the pendant droplet method and the Wilhelmy Plate method, respectively. According to Radiom et al. (2009), the decrease in surface tension is due to a decrease in cohesive energy at the liquid-air interface since Brownian motion brings nano-sized particles to the lowest level of interfacial energy.

3.4 Stability of flooding fluids

Nanoparticles agglomerate easily in the based fluid due to their large surface area and high surface energy, and their density becomes greater than the base solution, forcing nanoparticles to settle. As a result, it is critical to comprehend the mechanism of nanoparticle settlement.

According to the methods introduced in Section 2.3, three solutions of 0.5 wt% SiO_2 , 0.5 wt% TiO_2 , and hybrid (0.5 wt% TiO_2 + 0.5 wt% SiO_2) nanofluids were prepared (Fig. 3). Nanofluids were placed in a test tube at room temperature (25 °C) for 228 h.

As shown in Fig. 3, TiO_2 nanofluid is extremely unstable with a noticeable amount of nanoparticles settled. In Fig. 3(b), it can be observed that all TiO_2 nanoparticles settled at the

bottom of the transparent container (at $t = 96$ h). Hybrid nanofluid is relatively more stable than TiO_2 nanofluid, and no visible stratification was found even after 36 hours. After 48 hours, the solution began to stratify from top to bottom, with visually noticeable layers forming. SiO_2 nanofluid is the most stable, and there is no visible stratification during the experimental period (Fig. 3(c)).

TiO_2 nanoparticles are larger in size compared to SiO_2 nanoparticles. It is known that when particle size is larger, the attraction between particles is stronger, leading to faster agglomeration. Therefore, TiO_2 nanoparticles are subjected to a higher settling velocity. Additionally, TiO_2 nanoparticles are denser than SiO_2 nanoparticles, the gravitational effect is more pronounced as well. The TiO_2 nanoparticles used in the experiment are treated with a hydrophilic coating, hence having a large number of hydroxyl groups on the surface. The accumulation of nanoparticles is a complicated process driven by various factors such as particle size, surface charge, and density. All those reasons lead to faster agglomeration of TiO_2 nanoparticles compared to SiO_2 nanoparticles.

3.5 Measurement of contact angles

Li et al. (2017) defined contact angle θ in the 3-phase system, water, oil, and solid surface (Fig. 4) as follows in Table 7: water-wet with a contact angle in the range of 0-75°,

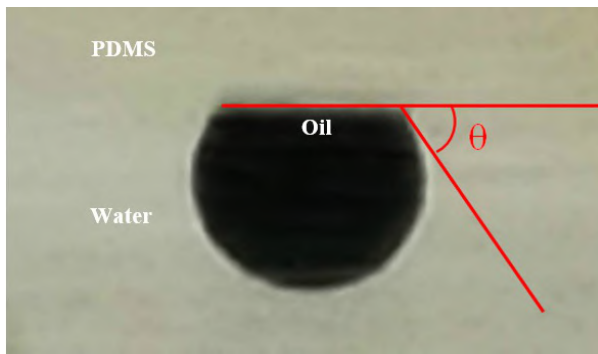


Fig. 4. Contact angle in the 3-phase system.

Table 7. Definition of wettability in a 3-phases system.

Contact angle (°)	Wettability
0–75	Water-wet
75–105	Intermediate/Neutral-wet
105–180	Oil-wet

intermediate/neutral-wet with a contact angle in the range of 75–105° and oil-wet with a contact angle in the range of 105–180°.

Contact angles for different nanofluids are measured and reported in Table 8. It can be observed that in the case of NaCl solution, the contact angle slightly increased compared to DI-water, and nanofluid tends to decrease the contact angle in both water-wet and oil-wet conditions. In our previous paper (Goharzadeh and Fatt, 2022), we reported the process for preparing transparent microchannels having water-wet or neutral-wet characteristics. The wettability of the polydimethylsiloxane (PDMS) microchannel changes with time when its surface is treated with plasma. A few minutes after the plasma cleaning process, DI-water and NaCl solution will keep the surface of the PDMS in a weakly water-wet condition. After 4 days, because of aging, the surface becomes oil-wet. On the other hand, contact with nanofluid can result in a water-wet condition, and the surface becomes neutral-wet after 4 days (Goharzadeh and Fatt, 2022).

3.6 Effect of flowrates on EOR process

To quantify the effect of flowrate on oil recovery after breakthrough, the flooding process is divided into three stages according to the flowrate (Table 9).

By calculating the ratio of oil recovery at each stage to total oil recovery, the effect of flowrate on oil recovery can be obtained. Fig. 5 shows that during the water, SiO₂ nanofluid, TiO₂ nanofluid, and TiO₂–SiO₂ hybrid nanofluid flooding, the oil is recovered in each stage. Almost 55%-65% of crude oil has been pushed out in the first stage; about 23%-29% of crude oil has been displaced out in the second stage; and in the third stage, corresponding to the maximum flowrate, very little additional oil is displaced. This oil recovery behavior implies that with the increase in flowrate, the flooding efficiency began

Table 8. Contact angle between different working fluids after plasma treatment of PDMS microchannel.

Working fluid	Contact angle (°)	
	Water wet	Neutral wet
DI-water	54.9	110.3
NaCl solution	57.5	120.8
SiO ₂ + brine	17.6	87.3
TiO ₂ + brine	13-23	71-81
TiO ₂ –SiO ₂ + brine	38-48	80-90

Table 9. Definition of each stage.

Stage	Flowrate (mL/h)
First	0.01-0.04
Second	0.05-0.07
Third	0.08-0.1

to decline. In the beginning, as the injection rate increases, the viscous forces between oil and nanofluid also increase. Accordingly, the oil recovery increases. However, if the flowrate effect is the primary displacement mechanism in the flooding process after breakthrough, then as the injection rate increases, the oil recovery should also increase according to Darcy's Law (Mai and Kantzas, 2009). The fact that this did not occur suggests that the oil recovered following the breakthrough is not flowrate-dependent. For water-wet condition, Roof (1970) observed that during water injection, the amount of water film around the pore surface increases and leads to water bridging at the pore throat. These water bridges will trap oil ganglia within the pore, and they will become stable and not be affected by the increase in flowrate after the breakthrough.

3.7 Effect of nanofluids on EOR process

The residual coefficient (Rc) is used to compare the displacement effect of oil ganglia during the flooding process after the breakthrough and is defined by:

$$R_c = \frac{\text{Oil saturation in each flowrate}}{\text{Oil saturation after initial flooding}} \quad (1)$$

In this experiment, the flowrate increased by 0.01 mL/h every 6 minutes, and the residual coefficient was measured for different nanofluids and presented as a function of pore volume (Fig. 6). It can be observed that at a low flowrate, the residual coefficient has almost the same value. However, as the pore volume increases in the system, the residual coefficient diverges between different solutions. The residual coefficient of SiO₂ nanofluid flooding reaches its lowest value of 0.45 at a pore volume of 60. This result shows that almost 60% of oil is removed after the breakthrough, and SiO₂ nanofluid represents the best candidate for the neutral-wet condition. For water-wet conditions, the recovery effect of hybrid nanofluids is better than that of SiO₂ and TiO₂ nanofluids, particularly for higher

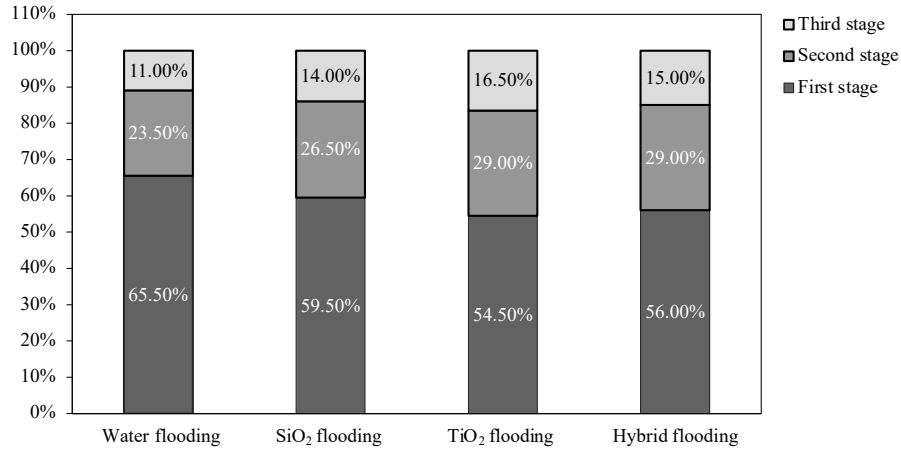


Fig. 5. Performance of working fluid in each stage.

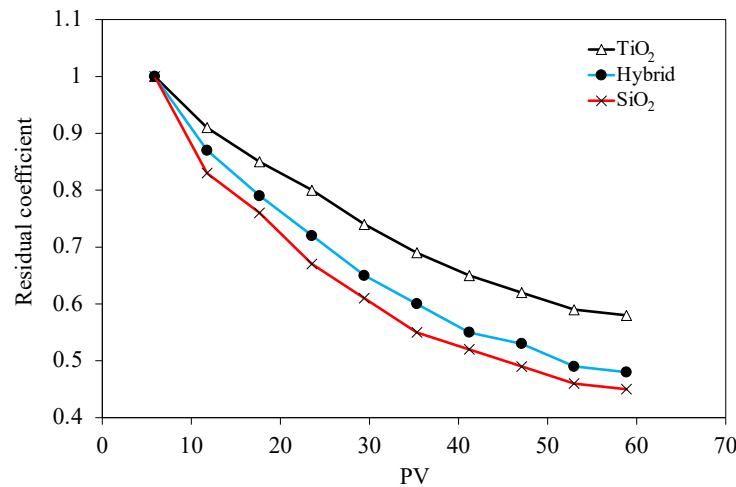


Fig. 6. Recovery effect of different nanofluids in neutral-wet condition (PV represents the pore volume injected).

pore volumes (Fig. 7). It can be observed that in a water-wet condition, 50% of oil is removed after the breakthrough of the hybrid nanofluids.

It is found in Section 3.2 that the dynamic viscosities of SiO₂, TiO₂, and hybrid nanofluids are comparable. However, SiO₂ nanofluid is the appropriate candidate for the EOR process in a neutral-wet condition, and hybrid nanofluid has the best efficiency in a water-wet condition. We conclude that viscosity and flowrates are not the key parameters for these obtained results, and it is therefore important to investigate the effect of surface tension and contact angles on the recovery effect.

4. Discussions

As we described in our previous study (Goharzadeh and Fatt, 2022), the Ca is a dimensionless number defined as the ratio of viscous force to capillary force. It reflects the equilibrium relationship between different forces in the process of two-phase flooding in the porous media, and it is an essential concept of the oil recovery mechanism (Liu et al., 2019). It is defined as:

$$Ca = \frac{\mu v}{\sigma \cos \theta} \quad (2)$$

where μ is the dynamic viscosity, v is a characteristic velocity, σ is the interfacial tension between two immiscible fluids, and θ is the contact angle. The recovery rate increases with increasing Ca. According to Eq. (2), to increase the capillary number, one should increase the injection rate or the viscosity of the flooding fluid, reduce the interfacial tension between two phases, or alter the contact angle.

Table 10 shows a summary of the results obtained in this study. If we compare the properties of SiO₂ with TiO₂ nanofluids, it can be easily concluded that SiO₂ nanofluid is the best candidate for an oil recovery process because its nanoparticles have a smaller size, the solution is stable, and the contact angle is the highest for both neutral and water-wet conditions.

Furthermore, TiO₂-SiO₂ hybrid nanofluid has even better properties for the oil recovery process (Table 10). The surface tension is decreased for approximately constant viscosity, and the contact angle of hybrid fluid is increased under both conditions, especially under water-wet conditions. The latest result suggests that hybrid nanofluid changes the wettability of

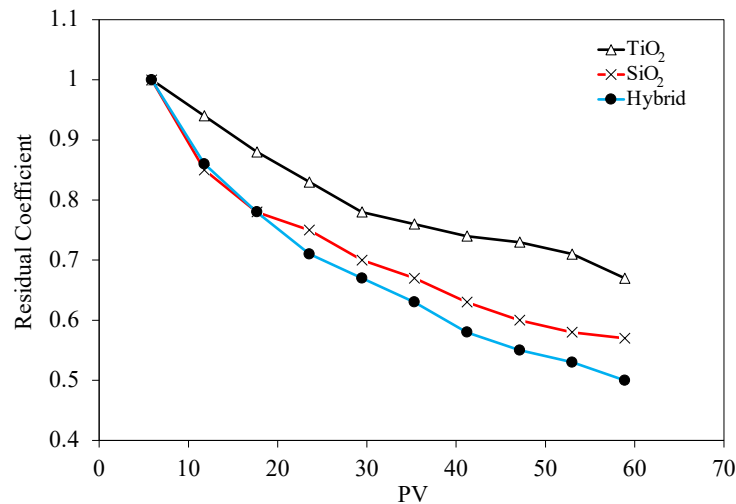


Fig. 7. Recovery effect of different nanofluids in water-wet condition (PV represents the pore volume injected).

Table 10. Summary of physical properties of nanofluids.

Fluid Type	Size (nm)	μ (mPa.s)	ρ (g/cm ³)	σ (mN/m)	Stability	Q (ml/h)	θ (°) NW	Ca (10 ⁻⁶) NW	θ (°) WW	Ca (10 ⁻⁶) WW
SiO ₂ + brine	187	1.03	1.0198	76.76	Very stable	No effect	87.3	5.69	17.6	0.28
TiO + brine	1,131	0.98	1.0201	72.67	Not stable	No effect	71-81	1.11	13-23	0.28
TiO ₂ -SiO ₂ + brine	917.8	1.01	1.0206	72.38	Stable	No effect	80-90	3.2	38-48	0.38

the porous matrix, bringing it closer to an oil-wetting porous medium. This result might explain why hybrid nanofluids perform better in water-wet conditions. In addition, the solution is more stable than TiO₂ nanofluid because the size of hybrid nanoparticles is smaller than TiO₂ nanoparticles, and therefore their settling time is longer than TiO₂. The capillary number is calculated for a constant velocity of 0.02 mm/s, and reported in Table 10. Under neutral-wet and water-wet conditions, the SiO₂ nanofluid and hybrid nanofluid, respectively, have the highest capillary numbers. These results show that the capillary number has a significant impact on the efficiency of the nanofluid flooding process. As the capillary number rises, the flooding efficiency increases. For constant flowrate and viscosity, increasing the capillary number requires either lowering the surface tension or increasing the contact angle.

5. Conclusions

The physical properties of TiO₂-SiO₂ hybrid nanofluid are characterized in this study. When nanoparticles are added to the brine solution, the average size of aggregated particles, the viscosity, the surface tension, the stability, and the contact angle of the obtained solution are altered. When TiO₂ and SiO₂ nanoparticles are added simultaneously to brine solution, the viscosity of the mixtures remains constant compared with nanofluids with single type nanoparticles, but the stability and contact angle increase. For neutral-wet and water-wet surface conditions, SiO₂ nanofluid and TiO₂-SiO₂ hybrid nanofluid flooding, respectively, produce the best recovery processes. Due to their large particle size, TiO₂ nanoparticles sediment,

and the nanofluid is unstable and therefore cannot be used for flooding process by itself. We conclude that the combination of the fluid's stability, wettability of the porous wall, surface tension, and contact angle of the three phases (crude oil-nanofluid solution-solid surface), constitute the key physical parameters in EOR using nanofluids, and the effects of flowrates and viscosity are negligible. The TiO₂-SiO₂ hybrid nanofluid has a lower surface tension while having a higher contact angle and better stability. If all physical parameters are set properly, the hybrid nanofluid becomes a good candidate for EOR processes in addition to its useful thermal characteristics identified in earlier studies. Future experiments will focus on how the concentration of nanoparticles in nanofluids influences the flooding process.

Acknowledgements

Mr. Fan Xue's assistance with the experimental measurements is greatly appreciated.

Conflict of interest

The authors declare no competing interest.

Open Access This article is distributed under the terms and conditions of the Creative Commons Attribution (CC BY-NC-ND) license, which permits unrestricted use, distribution, and reproduction in any medium, provided the original work is properly cited.

References

Ali, J. A., Kolo, K., Manshad, A. K., et al. Emerging applications of TiO₂/SiO₂/poly(acrylamide) nanocomposites

- within the engineered water EOR in carbonate reservoirs. *Journal of Molecular Liquids*, 2021, 322: 114943.
- Alomair, O. A., Matar, K. M., Alsaeed, Y. H. Nanofluids application for heavy oil recovery. Paper SPE 171539 Presented at the SPE Asia Pacific Oil & Gas Conference and Exhibition, Adelaide, Australia, 14-16 October, 2014.
- Alwated, B., El-Amin, M. F. Enhanced oil recovery by nanoparticles flooding: From numerical modeling improvement to machine learning prediction. *Advances in Geo-Energy Research*, 2021, 5(3): 297-317.
- Azmi, W. H., Hamid, K. A., Ramadhan, A. I., et al. Thermal hydraulic performance for hybrid composition ratio of TiO_2 - SiO_2 nanofluids in a tube with wire coil inserts. *Case Studies in Thermal Engineering*, 2021, 25: 100899.
- Bahrami, M., Akbari, M., Karimipour, A., et al. An experimental study on rheological behavior of hybrid nanofluids made of iron and copper oxide in a binary mixture of water and ethylene glycol: Non-Newtonian behavior. *Experimental Thermal and Fluid Science*, 2016, 79: 231-237.
- Chaturvedi, K. R., Narukulla, R., Sharma, T. Effect of single-step silica nanoparticle on rheological characterization of surfactant based CO_2 foam for effective carbon utilization in subsurface applications. *Journal of Molecular Liquids*, 2021, 341: 116905.
- Cheraghian, G., Rostami, S., Afrand, M. Nanotechnology in enhanced oil recovery. *Processes*, 2020, 8(9): 1073.
- Goharzadeh, A., Fatt, Y. Y. Combined effect of silica nanofluid and wettability on enhanced oil recovery process. *Petroleum Science and Engineering*, 2022, 215: 110663.
- Hamid, K. A., Azmi, W. H., Nabil, M. F., et al. Experimental investigation of thermal conductivity and dynamic viscosity on nanoparticle mixture ratios of TiO_2 - SiO_2 nanofluids. *International Journal of Heat and Mass Transfer*, 2018, 116: 1143-1152.
- Kashefi, F., Sabbaghi, S., Saboori, R., et al. Wettability alteration of sandstone oil reservoirs by different ratios of graphene oxide/silica hybrid nanofluid for enhanced oil recovery. *Journal of Dispersion Science and Technology*, 2023, in press, <https://doi.org/10.1080/01932691.2023.2204929>.
- Kazemzadeh, Y., Sharifi, M., Riazi, M., et al. Potential effects of metal oxide/ SiO_2 nanocomposites in EOR processes at different pressures. *Colloids and Surfaces A: Physicochemical and Engineering Aspects*, 2018, 559: 372-384.
- Li, R., Jiang, P., Gao, C., et al. Experimental investigation of silica-based nanofluid enhanced oil recovery: The effect of wettability alteration. *Energy & Fuels*, 2017, 31(1): 188-197.
- Li, K., Wang, D., Jiang, S. Review on enhanced oil recovery by nanofluids. *Oil & Gas Science and Technology—Revue d'IFP Energies nouvelles*, 2018, 73: 37.
- Liu, Y., Iglauer, S., Cai, J., et al. Local instabilities during capillary-dominated immiscible displacement in porous media. *Capillarity*, 2019, 2(1): 1-7.
- Liu, P., Mu, Z., Wang, C., et al. Experimental study of rheological properties and oil displacement efficiency in oilfields for a synthetic hydrophobically modified polymer. *Scientific Reports*, 2017, 7(1): 8791.
- Madhesh, D., Parameshwaran, R., Kalaiselvam, S. Experimental investigation on convective heat transfer and rheological characteristics of Cu-TiO_2 hybrid nanofluids. *Experimental Thermal and Fluid Science*, 2014, 52: 104-115.
- Mai, A., Kantzas, A. Heavy oil waterflooding: Effects of flowrate and oil viscosity. *Journal of Canadian Petroleum Technology*, 2009, 48: 42-51.
- McElfresh, P., Olguin, C., Ector, D. The application of nanoparticle dispersions to remove paraffin and polymer filter cake damage. Paper SPE 151848 Presented at the SPE International Symposium and Exhibition on Formation Damage Control, Lafayette, Louisiana, 15-17 February, 2012.
- Miller, R., Fainerman, V. The drop volume technique. *Studies in Interface Science*, 1998, 6: 139-186.
- Minea, A. A. Hybrid nanofluids based on Al_2O_3 , TiO_2 and SiO_2 : Numerical evaluation of different approaches. *International Journal of Heat and Mass Transfer*, 2017, 104: 852-860.
- Moghadasi, R., Rostami, A., Hemmati-Sarapardeh, A. Application of nanofluids for treating fines migration during hydraulic fracturing: Experimental study and mechanistic understanding. *Advances in Geo-Energy Research*, 2019, 3(2): 198-206.
- Mukherjee, S., Mishra, P. C., Aljuwayhel, N. F., et al. Thermofluidic performance of SiO_2 - ZnO /water hybrid nanofluid on enhancement of heat transport in a tube: Experimental results. *International Journal of Thermal Sciences*, 2022, 182: 107808.
- Murshed, S. S., Tan, S. H., Nguyen, N. T. Temperature dependence of interfacial properties and viscosity of nanofluids for droplet-based microfluidics. *Journal of Physics D: Applied Physics*, 2008, 41(8): 085502.
- Nabil, M. F., Azmi, W. H., Hamid, K. A., et al. An experimental study on the thermal conductivity and dynamic viscosity of TiO_2 - SiO_2 nanofluids in water: Ethylene glycol mixture. *International Communications in Heat and Mass Transfer*, 2017, 86: 181-189.
- Negin, C., Ali, S., Xie, Q. Application of nanotechnology for enhancing oil recovery—A review. *Petroleum*, 2016, 2(4): 324-333.
- Radiom, M., Yang, C., Chan, W. K. Characterization of surface tension and contact angle of nanofluids. Paper SPIE 7522 Presented at the Fourth International Conference on Experimental Mechanics, Singapore, 18-20 November, 2009.
- Roof, J. G. Snap-off of oil droplets in water-wet pores. *SPE Journal*, 1970, 10(1): 85-90.
- Salem Ragab, A. M., Hannora, A. E. A comparative investigation of nanoparticle effects for improved oil recovery—experimental work. Paper SPE 175395 Presented at the SPE Kuwait Oil and Gas Show and Conference, Mishref, Kuwait, 11-14 October, 2015.
- Sircar, A., Rayavarapu, K., Bist, N., et al. Applications of nanoparticles in enhanced oil recovery. *Petroleum Research*, 2022, 7(1): 77-90.

- Sivasankaran, S., Bhuvaneshwari, M. Numerical study on influence of water-based hybrid nanofluid and porous media on heat transfer and pressure loss. *Case Studies in Thermal Engineering*, 2022, 34: 102022.
- Sun, X., Zhang, Y., Chen, G., et al. Application of nanoparticles in enhanced oil recovery: A critical review of recent progress. *Energies*, 2017, 10(3): 345.
- Suresh, S., Venkataraj, K. P., Selvakumar, P., et al. Synthesis of Al_2O_3 -Cu/water hybrid nanofluids using two-step method and its thermo-physical properties. *Colloids and Surfaces A: Physicochemical and Engineering Aspects*, 2011, 388(1-3): 41-48.
- Vafaei, S., Purkayastha, A., Jain, A., et al. The effect of nanoparticles on the liquid-gas surface tension of Bi_2Te_3 nanofluids. *Nanotechnology*, 2009, 20(18): 185702.
- Wilkinson, M. C., Kidwell, R. L. A mathematical description of the Harkins and Brown correction curve for the determination of surface and interfacial tensions. *Journal of Colloid and Interface Science*, 1971, 35(1): 114-119.
- Yarmand, H., Gharekhani, S., Shirazi, S. F. S., et al. Study of synthesis, stability and thermophysical properties of graphene nanoplatelet/platinum hybrid nanofluid. *International Communications in Heat and Mass Transfer*, 2016, 77: 15-21.
- Yu, W., Xie, H. A review on nanofluids: Preparation, stability mechanisms, and applications. *Journal of Nanomaterials*, 2012, 2012: 435873.
- Yuan, L., Zhang, Y., Dehghanpour, H. A theoretical explanation for wettability alteration by adding nanoparticles in oil-water-tight rock systems. *Energy & Fuels*, 2021, 35(9): 7787-7798.
- Zainon, S. N. M., Azmi, W. H. Stability and thermo-physical properties of green bio-glycol based TiO_2 - SiO_2 nanofluids. *International Communications in Heat and Mass Transfer*, 2021, 126: 105402.
- Zhuang, Y., Goharzadeh, A., Lin, Y. J., et al. Three-dimensional measurements of asphaltene deposition in a transparent micro-channel. *Journal Petroleum Science and Engineering*, 2016, 145: 77-82.
- Zhuang, Y., Goharzadeh, A., Lin, Y. J., et al. Experimental study of asphaltene deposition in transparent microchannels using light absorption method. *Journal of Dispersion Science and Technology*, 2018, 39(5): 744-753.